18F-FDG PET in Posterior Cortical Atrophy and Dementia with Lewy Bodies

Jennifer L. Whitwell[1], Jonathan Graff-Radford[2], Tarun D. Singh[2], Daniel A. Drubach[2], Matthew L. Senjem[1,3], Anthony J. Spychalla[1], Nirubol Tosakulwong[4], Val J. Lowe[1], and Keith A. Josephs[2]

[1]Department of Radiology, Mayo Clinic, Rochester, Minnesota; [2]Department of Neurology, Mayo Clinic, Rochester, Minnesota; [3]Department of Information Technology, Mayo Clinic, Rochester, Minnesota; and [4]Department of Health Sciences Research (Biostatistics), Mayo Clinic, Rochester, Minnesota

Posterior cortical atrophy (PCA) and dementia with Lewy bodies (DLB) have both been associated with occipital lobe hypometabolism on 18F-FDG PET, whereas relative sparing of posterior cingulate metabolism compared with precuneus/cuneus (i.e., cingulate island sign) is a feature of DLB. We aimed to determine whether patterns of hypometabolism or the cingulate island sign differed between PCA and DLB. **Methods:** Sixteen clinically diagnosed PCA and 13 probable DLB subjects underwent 18F-FDG PET. All PCA subjects showed β-amyloid deposition on PET scanning. Regional hypometabolism was assessed compared with a control cohort (*n* = 29) using voxel- and region-level analyses in statistical parametric mapping. A ratio of metabolism in the posterior cingulate to precuneus plus cuneus was calculated to assess the cingulate island sign. In addition, the 18F-FDG PET scans were visually assessed to determine whether the cingulate island sign was present in each subject. **Results:** PCA and DLB showed overlapping patterns of hypometabolism involving the lateral occipital lobe, lingual gyrus, cuneus, precuneus, posterior cingulate, inferior parietal lobe, supramarginal gyrus, striatum, and thalamus. However, DLB showed greater hypometabolism in the medial occipital lobe, orbitofrontal cortex, anterior temporal lobe, and caudate nucleus than PCA, and PCA showed more asymmetric patterns of hypometabolism than DLB. The cingulate island sign was present in both DLB and PCA, although it was more asymmetric in PCA. **Conclusion:** Regional hypometabolism overlaps to a large degree between PCA and DLB, although the degree of involvement of the frontal and anterior temporal lobes and the presence of asymmetry could be useful in differential diagnosis.

Key Words: 18F-FDG PET; posterior cortical atrophy; dementia with Lewy bodies; cingulate island sign

Posterior cortical atrophy (PCA) and dementia with Lewy bodies (DLB) are 2 neurodegenerative diseases that have both been associated with hypometabolism on 18F-FDG PET in the occipital lobe. Patients with PCA present with a progressive decline in visuospatial and visuoperceptual deficits, with patients often having features of simultanagnosia, optic ataxia, oculomotor apraxia, and dysgraphia (*1*). In contrast, patients with DLB present with fluctuating cognitive impairment; recurrent visual hallucinations; features of parkinsonism, such as bradykinesia, rigidity, resting tremor, and postural instability; and rapid eye movement sleep behavior disorder (RBD) (*2*). Despite these differing clinical presentations, studies have reported similar patterns of hypometabolism on 18F-FDG PET, with both associated with hypometabolism predominantly in the occipital and temporoparietal cortices (*3–9*). In fact, the presence of occipital hypometabolism has been shown to be a useful feature to differentiate both DLB (*8,10–12*) and PCA (*4–6*) from typical Alzheimer dementia. There is often some overlap in the clinical presentation of these diseases, with, for example, hallucinations and RBD sometimes occurring in PCA patients (*3,13*), and so additional biomarkers that can help the differential diagnosis would be of value. It is currently unclear whether patterns of hypometabolism on 18F-FDG PET could be useful in this regard.

In addition to a characteristic pattern of occipital hypometabolism, studies in DLB have noted that the posterior cingulate is relatively spared and that a ratio of hypometabolism of the posterior cingulate to the precuneus plus cuneus (i.e., the cingulate island sign [CIS]) can differentiate DLB from typical Alzheimer dementia with high accuracy (*14–16*). It is unclear, however, whether the CIS is also a feature of PCA. The presence of the CIS is associated with lower Braak stages (*14,17*), and hence one could hypothesize that it may help differentiate DLB from PCA, because PCA is often associated with Alzheimer disease pathology and high Braak stage (*1*).

The aim of this study was, therefore, to compare patterns of hypometabolism on 18F-FDG PET, including an assessment of the CIS, in PCA and DLB to determine whether there are any potentially diagnostically useful differences.

MATERIALS AND METHODS

Subjects

Sixteen patients fulfilling clinical criteria for PCA (*1,3*) and 13 patients fulfilling clinical criteria for probable DLB (*2*) were recruited from the Department of Neurology, Mayo Clinic, and underwent 18F-FDG PET between 2010 and 2015. All patients had been evaluated by 1 of 2 behavioral neurologists. Neuroimaging findings were not used in the diagnosis of either DLB or PCA. The PCA inclusion criteria (*3*) were insidious onset and gradual progression; presentation of visual complaints in the absence of significant primary ocular disease explaining the symptoms; relative preservation of anterograde memory and insight early in the disorder; disabling visual impairment

throughout the disorder; and presence of any of the following: simultanagnosia with or without optic ataxia or oculomotor apraxia, constructional dyspraxia, visual field defect, environmental disorientation, or any elements of Gerstmann syndrome (acalculia, agraphia, left-right disorientation, and finger agnosia). Clinical PCA features that were recorded in each subject included simultagnosia, optic ataxia, oculomotor apraxia, and dysgraphia (3). The presence of simultanagnosia was assessed using the Ishihara color plates and the documentation of how many items were recognized on visual inspection of a picture with 5 overlapping items. Cutoff was below 6 of 6 for plates and below 5 of 5 on overlapping pictures based on performance of 10 controls who scored 100% on both tests. Handwriting samples were assessed for evidence of dysgraphia (3). The presence or absence of oculomotor apraxia and optic ataxia was assessed on neurologic examination. Oculomotor apraxia was defined as the inability to voluntarily direct one's gaze to a particular point. Optic ataxia was defined as the impairment of goal-directed hand movements toward visually presented targets. Clinical DLB features that were recorded in each subject included fluctuations, parkinsonism, visual hallucinations, and RBD. RBD was considered present if the behavior met diagnostic criteria B for RBD, defined as abnormal, wild flailing movements occurring during sleep (with sleep-related injuries), or movements that are potentially injurious or disruptive (18). Visual hallucinations were defined as a false visual perception, not associated with real external stimuli and not associated with falling or awakening from sleep, and had to be well formed, recurrent, well documented, nonfleeting, and spontaneous.

All 16 PCA subjects had undergone β-amyloid PET imaging using Pittsburgh compound B and were β-amyloid–positive (19). One PCA subject has died and was found to have Alzheimer disease at autopsy (Braak stage VI). The study was approved by the Mayo Clinic Institutional Review Board, and all patients consented to research.

The PCA and DLB subjects were matched 1:1 to 29 healthy control subjects who had undergone ^{18}F-FDG PET (median age at PET, 66 y [interquartile range, 61–70 y], 31% women). All healthy controls had been recruited into the Mayo Clinic Study of Aging, and subjects were characterized as cognitively normal by consensus (20,21) and when their age-adjusted neuropsychologic test scores were consistent with normative data developed in this community (22). Imaging findings were not used in the diagnosis of controls.

^{18}F-FDG PET Analysis

All subjects underwent ^{18}F-FDG PET performed using a PET/CT scanner (GE Healthcare) operating in 3-dimensional mode. Subjects were injected with ^{18}F-FDG (average, 459 MBq [range, 367–576 MBq]) and after injection were allowed to wait in a comfortable chair for the 30-min uptake period, in a dimly lit room, without talking, moving, or sleeping. After the 30-min uptake period, an 8-min ^{18}F-FDG scan was obtained consisting of four 2-min dynamic frames after a low-dose CT transmission scan. Individual frames of the dynamic series were realigned if motion was detected, and then a mean image was created. All subjects had also undergone a volumetric MRI scan at the same time as the ^{18}F-FDG PET scan, using a standardized protocol (19).

Voxel-level and region-level analyses were used to assess ^{18}F-FDG PET. The voxel-level analysis was performed using statistical parametric mapping 5 (23). All MR images were normalized to a customized template (24). The PET images were coregistered to the patients' MR image using 6-degree-of-freedom registration. The automated anatomic labeling atlas, containing pons, was propagated to native MRI space. Partial-volume correction of cerebrospinal fluid and tissue compartments was applied through the 2-compartment model (25) to remove atrophy effects on the ^{18}F-FDG uptake. All voxels in the PET images were divided by median uptake of the pons to form ^{18}F-FDG uptake ratio images. The ^{18}F-FDG PET uptake ratio images were then normalized to the customized template using the normalization parameters from the MRI normalization. Group statistical comparisons were performed comparing PCA and DLB with each other and with the healthy control cohort, using 2-sided t tests. All comparisons were corrected for multiple comparisons using the false-discovery rate at a P value of less than 0.05. A conjunction analysis using the contrasts comparing each disease group with controls was performed to assess regions of hypometabolism that overlapped between PCA and DLB. Age and sex were included in all comparisons as covariates.

Atlas-based parcellation with the automated anatomic labeling atlas (26) was used to generate PET uptake of specific regions of interest. Partial-volume–corrected ^{18}F-FDG PET uptake ratios were calculated for the occipital (lateral occipital, cuneus, calcarine, lingual), parietal (inferior and superior parietal lobe, supramarginal gyrus, angular gyrus, precuneus, posterior cingulate), temporal (temporal pole, inferior, middle and superior temporal gyri, hippocampus, parahippocampal gyrus and fusiform gyrus) and frontal lobes (orbitofrontal and prefrontal cortex), and subcortical nuclei (caudate, putamen, and thalamus). Left and right hemisphere values were averaged for our group comparisons, because there was no evidence for any hemispheric differences at the group level. However, hemispheric asymmetry scores were also calculated for each subject as the absolute difference between left and right hemisphere.

The CIS was assessed using both a quantitative and a visual approach. The quantitative CIS was calculated by dividing the median uptake ratio in the posterior cingulate gyrus by the median uptake ratio in the precuneus plus cuneus (14,16). ^{18}F-FDG PET images were visually assessed, with the behavioral neurologist masked to clinical diagnosis, to determine whether a CIS was present in each subject based on the axial and sagittal raw ^{18}F-FDG PET images. A subject was considered to have a CIS if ^{18}F-FDG metabolism was lower in the precuneus and cuneus than in the posterior cingulate in either hemisphere, as previously described (14,16). A CIS was visually graded as asymmetric if a CIS was present in one hemisphere but not the other.

Statistical Analysis

Statistical analyses were performed using JMP computer software (version 10.0.0; SAS Institute Inc.) with significance assessed at a P value of 0.05 or less. χ^2 tests were used to compare categoric data, and Wilcoxon signed-rank tests were used to compare continuous data. Sensitivity, specificity, positive predictive value, and negative predictive value for differentiating PCA and DLB were calculated for variables that showed significant differences between PCA and DLB.

RESULTS

No differences were observed between PCA and DLB in age at scanning or degree of cognitive impairment (Table 1). However, PCA had a longer disease duration and younger age at onset than DLB.

PCA and DLB showed overlap in patterns of hypometabolism in the voxel-level maps when compared with controls (Fig. 1). Both groups showed hypometabolism in the bilateral lateral occipital lobe, lingual gyrus, cuneus, precuneus, posterior cingulate, inferior parietal lobe, left supramarginal gyrus, lateral posterior temporal lobes, and thalamus. In addition to these common regions, DLB showed hypometabolism throughout the frontal lobes and basal ganglia (Fig. 1). On direct comparison, DLB showed greater hypometabolism throughout the frontal and anterior

TABLE 1
Subject Demographics and Clinical Features

Demographic	PCA ($n = 16$)	DLB ($n = 13$)	P
Sex (% female)	7 (44%)	2 (15%)	0.10
Age at onset (y)	60.5 (54.0–63.8)	66 (61.5–70.0)	0.005
Age at ^{18}F-FDG (y)	64.0 (58.0–70.0)	68.0 (64.0–71.5)	0.15
Disease duration	4 (3.3–6.5)	3 (2–4)	0.006
Handedness (right)	15 (94%)	13 (100%)	0.27
Mini-Mental State Examination (/30)	25.5 (21.8–28.0)	25.0 (18.5–25.8)	0.32
Clinical features (%)			
Optic ataxia	3 (21%)*	0 (0%)	0.04
Simultanagnosia	12 (86%)*	0 (0%)	<0.0001
Oculomotor apraxia	7 (50%)*	0 (0%)	0.001
Dysgraphia	10 (63%)	0 (0%)	<0.0001
Hallucinations	4 (25%)	7 (54%)	0.11
Fluctuations	0 (0%)	12 (92%)	<0.0001
Parkinsonism	2 (12.5%)	13 (100%)	<0.0001
Rapid eye movement sleep behavior disorder	3 (19%)	10 (77%)	0.001

*Clinical features were assessed in 14 PCA subjects.
Data are median, with interquartile range in parentheses, or number, with percentage in parentheses.

temporal lobes than PCA (Fig. 1). No regions showed greater hypometabolism in PCA than DLB.

In the region-of-interest analysis both groups showed hypometabolism across many of the regions compared with controls, although DLB showed greater hypometabolism in calcarine gyrus, lingual gyrus, temporal pole, orbitofrontal cortex, prefrontal cortex, and caudate than PCA (Table 2). Hemispheric asymmetry in the occipital and parietal lobes was greater in PCA than in controls and DLB, and in the temporal lobe it was greater in PCA than in controls (Table 2). Of the 16 PCA subjects, 15 (94%) showed asymmetry in either the parietal or the occipital lobe (with asymmetry scores greater than the maximum value in controls). Ten of these showed greater hypometabolism in the right than in the left hemisphere, and 5 showed greater hypometabolism in the left than in the right. Only 4 DLB subjects (31%) showed evidence for asymmetry.

There was a trend for the quantitative CIS to be higher in subjects with DLB than in controls ($P = 0.09$), but no differences were observed between PCA and controls ($P = 0.43$) or between PCA and DLB ($P = 0.43$) (Table 2). Visual assessment identified the CIS in 11 of 13 (85%) of the DLB subjects and in 8 of 16 (50%) of the PCA subjects ($P = 0.05$). However, it was found that the CIS was more commonly asymmetric in the PCA subjects (5/8, 63%) compared with the DLB subjects (1/11, 9%, $P = 0.01$) (Fig. 2). Of the 5 asymmetric PCA cases, 3 showed a CIS in the right hemisphere and 2 in the left hemisphere. The 1 asymmetric DLB subject showed a CIS in the right hemisphere.

The presence of an asymmetric CIS showed high specificity for PCA (92%) but low sensitivity (31%) (Table 3). However, the presence of asymmetry in the parietal or occipital lobe showed high sensitivity (94%) and good specificity (69%) for a diagnosis of PCA. The variables that performed the best in predicting DLB
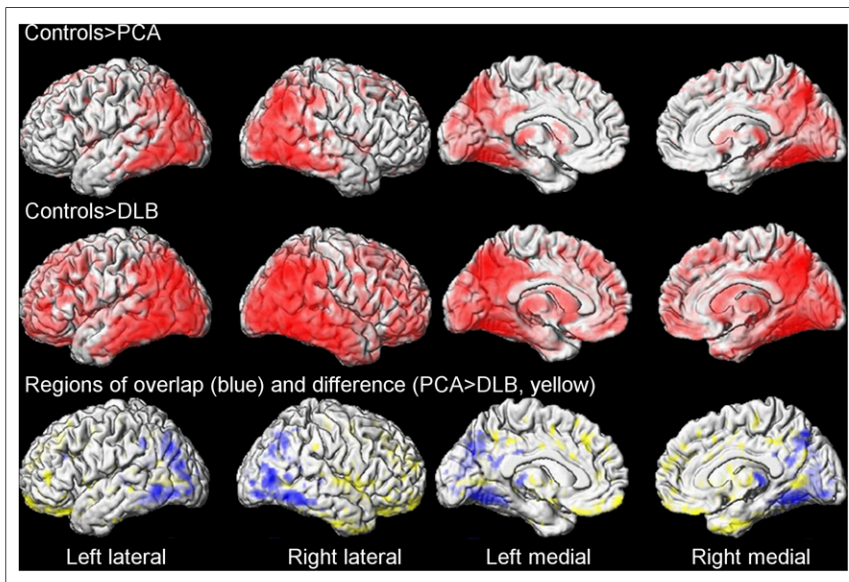

FIGURE 1. Regional ^{18}F-FDG PET hypometabolism in PCA and DLB compared with controls. (Top and middle) Regions of overlap between PCA and DLB using conjunction analysis (blue) and regions that showed greater hypometabolism in DLB than PCA on direct comparison (yellow) (bottom). Results shown after correction for multiple comparisons at $P < 0.05$.

TABLE 2
Regional ^{18}F-FDG SUVRs

Region	Controls	PCA	DLB	PCA vs. DLB P
Occipital lobe				
Lateral occipital gyrus	1.78 (1.62–1.83)	1.26 (1.19–1.46)*	1.31 (1.25–1.41)*	0.47
Cuneus	1.95 (1.75–2.02)	1.60 (1.51–1.82)*	1.61 (1.48–1.66)*	0.71
Calcarine gyrus	2.02 (1.89–2.13)	1.80 (1.68–1.97)*	1.65 (1.52–1.75)*	0.01
Lingual gyrus	1.84 (1.68–1.91)	1.64 (1.50–1.75)*	1.46 (1.43–1.53)*	0.02
Occipital asymmetry†	0.02 (0.01–0.03)	0.12 (0.07–0.14)*	0.06 (0.01–0.10)	0.02
Parietal lobe				
Inferior parietal lobe	2.00 (1.89–2.10)	1.51 (1.33–1.66)*	1.45 (1.31–1.65)*	0.84
Superior parietal lobe	2.01 (1.94–2.16)	1.55 (1.40–1.62)*	1.51 (1.38–1.68)*	0.97
Supramarginal gyrus	1.75 (1.69–1.84)	1.46 (1.33–1.62)*	1.43 (1.36–1.52)*	0.28
Angular gyrus	1.92 (1.81–2.03)	1.34 (1.26–1.49)*	1.33 (1.19–1.40)*	0.34
Precuneus	1.98 (1.82–2.07)	1.51 (1.37–1.65)*	1.51 (1.37–1.57)*	0.87
Posterior cingulate	1.72 (1.59–1.83)	1.44 (1.33–1.61)*	1.46 (1.41–1.59)*	0.68
Parietal asymmetry†	0.04 (0.02–0.07)	0.14 (0.09–0.18)*	0.05 (0.04–0.07)	0.005
Temporal lobe				
Temporal pole	1.45 (1.40–1.51)	1.43 (1.34–1.52)	1.34 (1.30–1.37)*	0.007
Inferior temporal gyrus	1.62 (1.57–1.68)	1.33 (1.24–1.45)*	1.29 (1.25–1.35)*	0.32
Middle temporal gyrus	1.67 (1.60–1.73)	1.34 (1.23–1.45)*	1.28 (1.20–1.42)*	0.48
Superior temporal gyrus	1.68 (1.60–1.75)	1.51 (1.42–1.59)*	1.44 (1.39–1.53)*	0.17
Hippocampus	1.23 (1.20–1.26)	1.19 (1.14–1.32)	1.25 (1.18–1.27)	0.65
Parahippocampal gyrus	1.32 (1.30–1.40)	1.27 (1.17–1.37)	1.23 (1.18–1.27)*	0.43
Fusiform gyrus	1.52 (1.47–1.60)	1.27 (1.23–1.41)*	1.29 (1.27–1.37)*	0.59
Temporal asymmetry†	0.02 (0.01–0.03)	0.06 (0.03–0.09)*	0.04 (0.01–0.06)	0.11
Frontal lobe				
Orbitofrontal cortex	1.82 (1.75–1.91)	1.77 (1.66–1.87)	1.64 (1.56–1.68)*	0.003
Prefrontal cortex	1.85 (1.78–1.20)	1.73 (1.63–1.83)*	1.65 (1.52–1.71)*	0.04
Frontal asymmetry†	0.04 (0.03–0.06)	0.03 (0.02–0.08)	0.04 (0.02–0.09)	0.65
Subcortical				
Caudate	1.55 (1.53–1.60)	1.48 (1.42–1.59)	1.40 (1.35–1.43)*	0.02
Putamen	1.55 (1.49–1.61)	1.49 (1.39–1.56)*	1.45 (1.41–1.52)*	0.45
Thalamus	1.59 (1.53–1.67)	1.47 (1.42–1.52)*	1.43 (1.40–1.46)*	0.13
Subcortical asymmetry†	0.03 (0.02–0.04)	0.03 (0.01–0.04)	0.02 (0.01–0.05)	0.77
CIS	0.91 (0.87–0.93)	0.91 (0.86–0.98)	0.94 (0.88–1.03)	0.43

*Significant difference from controls at $P < 0.05$.
†Asymmetry scores calculated as absolute difference between left and right hemisphere SUVRs.
Data shown are median, with interquartile range in parentheses.

were hypometabolism in the temporal pole and orbitofrontal cortex (Table 3).

DISCUSSION

This study demonstrates that PCA and DLB have strikingly similar patterns of hypometabolism involving the posterior cortices of the brain. However, DLB tended to show more severe and widespread patterns of dysfunction, whereas PCA showed more asymmetric patterns of hypometabolism. The CIS was present in both groups, although a symmetric CIS was more suggestive of DLB and an asymmetric CIS more suggestive of PCA. These findings could have clinical utility in helping to differentiate these diseases.

Hypometabolism in the occipital lobe, as well as parietal lobe, lateral temporal cortex, striatum, and thalamus, was observed in both PCA and DLB in our study, suggesting dysfunction to a common network of structures. One could hypothesize that dysfunction in this network of structures may contribute to the overlapping features observed across PCA and DLB. Occipital hypometabolism has been associated with the presence of DLB clinical features (27–29), and visual hallucinations, parkinsonism, and RBD were observed in some of our PCA patients, as has previously been reported (13). Atrophy of the primary visual cortex and thalamus has indeed been associated with the presence of visual hallucinations in PCA (13), and parietal and thalamic atrophy has been associated with parkinsonism in PCA
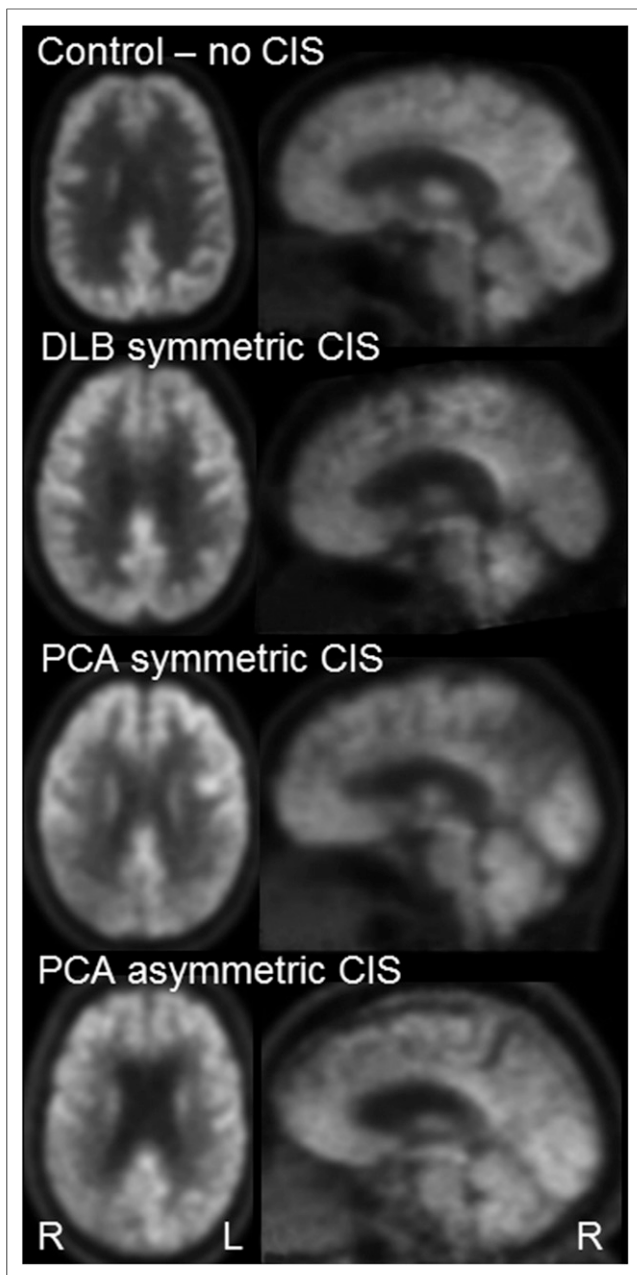
FIGURE 2. Example ^{18}F-FDG PET showing CIS in PCA and DLB.

(30). However, PCA patients showed striking visual impairments, such as simultanagnosia, oculomotor apraxia, and optic ataxia, which have also been linked to occipital–parietal hypometabolism *(3)*, that were not observed in DLB. Further work is therefore required to disentangle the neuroanatomic basis for the clinical differences between PCA and DLB within this network.

Some differences were observed between PCA and DLB in patterns of hypometabolism, with DLB tending to show more severe and widespread dysfunction than PCA. Notably, DLB showed greater hypometabolism in the medial occipital lobe, orbitofrontal cortex, prefrontal cortex, anterior temporal lobe, and caudate nucleus. This more widespread pattern of hypometabolism is similar to previous ^{18}F-FDG PET findings in DLB *(7,8,14)* and concurs with the idea that DLB is associated with a distributed pattern of network dysfunction, involving dorsal attention and executive networks *(31)*. Conversely, metabolism in the anterior temporal lobes and prefrontal cortices, with the exception of regions in the frontal eye fields, are typically spared in PCA *(3–5)*. Involvement of these structures on ^{18}F-FDG PET could therefore suggest a diagnosis of DLB. Hypometabolism of the orbitofrontal cortex and temporal pole showed particularly good sensitivity and specificity to differentiate DLB from PCA. Another striking difference between the 2 syndromes was the presence of asymmetry, which was observed in almost all PCA subjects but rarely observed in DLB. This asymmetry was not evident in the group comparisons because the PCA cohort consisted of some subjects with greater involvement of the right hemisphere and others with greater involvement of the left hemisphere, as others have observed *(32)*. However, the presence of asymmetry in either direction showed excellent sensitivity and specificity for a diagnosis of PCA and should therefore be considered in the differential diagnosis.

The CIS, showing relative sparing of the posterior cingulate compared with the precuneus and cuneus, was observed in most of the DLB subjects on visual inspection, supporting previous studies in DLB *(14,16,33)*. However, the quantitative CIS values did not differ between DLB and PCA, with half of the PCA subjects also showing a CIS on visual inspection, suggesting a CIS is not specific to DLB. It has been hypothesized that the CIS provides a marker of Alzheimer disease pathology *(14)*, whereby the absence of a CIS in Alzheimer dementia reflects hypometabolism of the posterior cingulate resulting from disrupted inputs from the hippocampus *(33,34)*. In contrast, the presence of a CIS in DLB reflects a low Braak stage *(14)*. This is not likely to be the case in PCA because all our PCA subjects showed positive β-amyloid PET scans, and PCA cases typically have a high Braak stage *(1)*. Instead, it likely reflects the fact that PCA subjects often have an unusual distribution of neurofibrillary tangles with relative sparing of the hippocampus *(1,35–37)*. Interestingly, the CIS in DLB has been associated with medial temporal lobe atrophy *(33)*. Therefore, the presence of CIS in DLB and PCA may indicate sparing of posterior limbic circuitry in both disorders compared with typical Alzheimer dementia. This also shows that the presence of posterior cingulate hypometabolism is not a reliable sign of the presence of Alzheimer disease when dealing with atypical clinical presentations. Although the CIS was also found in PCA, we did find a difference in the visual symmetry of the CIS in DLB and PCA. Although the DLB cases typically showed sparing of the posterior cingulate compared with the precuneus and cuneus in both hemispheres, a large proportion of PCA cases showed asymmetry, with the CIS often observed only in 1 hemisphere. This matches our finding of general asymmetry in PCA. The presence of an asymmetric CIS had excellent sensitivity for PCA because it was rarely observed in DLB, suggesting it could be a useful diagnostic clue for PCA. However, it had poor specificity and so the absence of an asymmetric CIS would not rule out the diagnosis of PCA.

A strength of our study is that our ^{18}F-FDG PET analyses were corrected for partial-volume averaging due to atrophy. This is a particularly important correction in this cohort because PCA is associated with striking cortical atrophy *(37)* whereas DLB is not typically associated with much atrophy *(38)*. We also had autopsy confirmation of Alzheimer disease in 1 PCA subject, and all PCA subjects underwent β-amyloid PET imaging in order to increase confidence that these subjects had underlying Alzheimer disease. The lack of β-amyloid PET imaging in the DLB

TABLE 3
Diagnostic Statistics to Differentiate PCA and DLB

Measure	Predicted group	Cutoff	Sensitivity	Specificity	Positive predictive value	Negative predictive value
Asymmetric CIS	PCA	+/−	0.31	0.92	0.83	0.43
Symmetric CIS	DLB	+/−	0.77	0.63	0.77	0.81
Occipital/parietal asymmetry*	PCA	+/−	0.94	0.69	0.79	0.90
Calcarine gyrus	DLB	1.75	0.79	0.69	0.69	0.79
Lingual gyrus	DLB	1.52	0.79	0.69	0.69	0.79
Temporal pole	DLB	1.39	0.92	0.72	0.69	0.93
Orbitofrontal cortex	DLB	1.68	0.80	0.73	0.75	0.79
Prefrontal cortex	DLB	1.79	0.89	0.62	0.50	0.93
Caudate	DLB	1.46	0.85	0.71	0.69	0.86

*Asymmetric = asymmetry score in either occipital or parietal lobe was > 0.09 (maximum in controls).

subjects is a limitation of the study given that DLB subjects can often have Alzheimer disease in addition to Lewy body pathology. However, both occipital hypometabolism and the CIS have been shown to be present in DLB independent of β-amyloid PET findings (12,14). Another potential limitation is that the PCA subjects had longer disease duration than the DLB subjects, which may have reduced power to detect regions with greater hypometabolism in DLB. We did not find any regions with greater hypometabolism in PCA than DLB, and this would likely be unchanged if we had a PCA cohort earlier in their disease course.

CONCLUSION

Our findings suggest that investigating patterns of hypometabolism on ^{18}F-FDG PET in subjects with a suspected diagnosis of PCA or DLB may be useful for differential diagnosis. The presence of hypometabolism in the orbitofrontal cortex and temporal pole, in addition to the typical pattern of occipital and parietal hypometabolism, would suggest a diagnosis of DLB, whereas the presence of asymmetric hypometabolism in the occipital and parietal lobes would be more indicative of a diagnosis of PCA.

DISCLOSURE

REFERENCES

1. Tang-Wai DF, Graff-Radford NR, Boeve BF, et al. Clinical, genetic, and neuropathologic characteristics of posterior cortical atrophy. *Neurology.* 2004; 63:1168–1174.
2. McKeith IG, Dickson DW, Lowe J, et al. Diagnosis and management of dementia with Lewy bodies: third report of the DLB Consortium. *Neurology.* 2005;65:1863–1872.
3. Singh TD, Josephs KA, Machulda MM, et al. Clinical, FDG and amyloid PET imaging in posterior cortical atrophy. *J Neurol.* 2015;262:1483–1492.
4. Nestor PJ, Caine D, Fryer TD, Clarke J, Hodges JR. The topography of metabolic deficits in posterior cortical atrophy (the visual variant of Alzheimer's disease) with FDG-PET. *J Neurol Neurosurg Psychiatry.* 2003;74:1521–1529.
5. Rosenbloom MH, Alkalay A, Agarwal N, et al. Distinct clinical and metabolic deficits in PCA and AD are not related to amyloid distribution. *Neurology.* 2011;76:1789–1796.
6. Wang XD, Lu H, Shi Z, et al. A pilot study on clinical and neuroimaging characteristics of Chinese posterior cortical atrophy: comparison with typical Alzheimer's disease. *PLoS One.* 2015;10:e0134956.
7. Claassen DO, Lowe VJ, Peller PJ, Petersen RC, Josephs KA. Amyloid and glucose imaging in dementia with Lewy bodies and multiple systems atrophy. *Parkinsonism Relat Disord.* 2011;17:160–165.
8. Minoshima S, Foster NL, Sima AA, Frey KA, Albin RL, Kuhl DE. Alzheimer's disease versus dementia with Lewy bodies: cerebral metabolic distinction with autopsy confirmation. *Ann Neurol.* 2001;50:358–365.
9. Spehl TS, Hellwig S, Amtage F, et al. Syndrome-specific patterns of regional cerebral glucose metabolism in posterior cortical atrophy in comparison to dementia with Lewy bodies and Alzheimer's disease: a [F-18]-FDG pet study. *J Neuroimaging.* 2015;25:281–288.
10. Albin RL, Minoshima S, D'Amato CJ, Frey KA, Kuhl DA, Sima AA. Fluorodeoxyglucose positron emission tomography in diffuse Lewy body disease. *Neurology.* 1996;47:462–466.
11. Gilman S, Koeppe RA, Little R, et al. Differentiation of Alzheimer's disease from dementia with Lewy bodies utilizing positron emission tomography with [18F]fluorodeoxyglucose and neuropsychological testing. *Exp Neurol.* 2005;191 (suppl 1):S95–S103.
12. Ishii K, Imamura T, Sasaki M, et al. Regional cerebral glucose metabolism in dementia with Lewy bodies and Alzheimer's disease. *Neurology.* 1998;51:125–130.
13. Josephs KA, Whitwell JL, Boeve BF, et al. Visual hallucinations in posterior cortical atrophy. *Arch Neurol.* 2006;63:1427–1432.
14. Graff-Radford J, Murray ME, Lowe VJ, et al. Dementia with Lewy bodies: basis of cingulate island sign. *Neurology.* 2014;83:801–809.
15. Imamura T, Ishii K, Sasaki M, et al. Regional cerebral glucose metabolism in dementia with Lewy bodies and Alzheimer's disease: a comparative study using positron emission tomography. *Neurosci Lett.* 1997;235:49–52.
16. Lim SM, Katsifis A, Villemagne VL, et al. The ^{18}F-FDG PET cingulate island sign and comparison to ^{123}I-beta-CIT SPECT for diagnosis of dementia with Lewy bodies. *J Nucl Med.* 2009;50:1638–1645.
17. Braak H, Braak E. Neuropathological staging of Alzheimer-related changes. *Acta Neuropathol (Berl).* 1991;82:239–259.
18. Sateia MJ, Reed VA, Christian Jernstedt G. The Dartmouth sleep knowledge and attitude survey: development and validation. *Sleep Med.* 2005;6:47–54.
19. Jack CR Jr, Lowe VJ, Senjem ML, et al. [11]C PiB and structural MRI provide complementary information in imaging of Alzheimer's disease and amnestic mild cognitive impairment. *Brain.* 2008;131:665–680.
20. Petersen RC, Roberts RO, Knopman DS, et al. Prevalence of mild cognitive impairment is higher in men: The Mayo Clinic Study of Aging. *Neurology.* 2010;75:889–897.
21. Roberts RO, Geda YE, Knopman DS, et al. The Mayo Clinic Study of Aging: design and sampling, participation, baseline measures and sample characteristics. *Neuroepidemiology.* 2008;30:58–69.

22. Harris ME, Ivnik RJ, Smith GE. Mayo's Older Americans Normative Studies: expanded AVLT recognition trial norms for ages 57 to 98. *J Clin Exp Neuropsychol.* 2002;24:214–220.

23. Ashburner J, Friston KJ. Voxel-based morphometry: the methods. *Neuroimage.* 2000;11:805–821.

24. Ashburner J, Friston KJ. Unified segmentation. *Neuroimage.* 2005;26:839–851.

25. Meltzer CC, Kinahan PE, Greer PJ, et al. Comparative evaluation of MR-based partial-volume correction schemes for PET. *J Nucl Med.* 1999;40:2053–2065.

26. Tzourio-Mazoyer N, Landeau B, Papathanassiou D, et al. Automated anatomical labeling of activations in SPM using a macroscopic anatomical parcellation of the MNI MRI single-subject brain. *Neuroimage.* 2002;15:273–289.

27. Fujishiro H, Iseki E, Kasanuki K, et al. Glucose hypometabolism in primary visual cortex is commonly associated with clinical features of dementia with Lewy bodies regardless of cognitive conditions. *Int J Geriatr Psychiatry.* 2012;27:1138–1146.

28. Firbank MJ, Lloyd J, O'Brien JT. The relationship between hallucinations and FDG-PET in dementia with Lewy bodies. *Brain Imaging Behav.* 2016;10:636–639.

29. Perneczky R, Drzezga A, Boecker H, Forstl H, Kurz A, Haussermann P. Cerebral metabolic dysfunction in patients with dementia with Lewy bodies and visual hallucinations. *Dement Geriatr Cogn Disord.* 2008;25:531–538.

30. Ryan NS, Shakespeare TJ, Lehmann M, et al. Motor features in posterior cortical atrophy and their imaging correlates. *Neurobiol Aging.* 2014;35:2845–2857.

31. Galvin JE, Price JL, Yan Z, Morris JC, Sheline YI. Resting bold fMRI differentiates dementia with Lewy bodies vs Alzheimer disease. *Neurology.* 2011;76:1797–1803.

32. Schmidtke K, Hull M, Talazko J. Posterior cortical atrophy: variant of Alzheimer's disease? A case series with PET findings. *J Neurol.* 2005;252:27–35.

33. Iizuka T, Kameyama M. Cingulate island sign on FDG-PET is associated with medial temporal lobe atrophy in dementia with Lewy bodies. *Ann Nucl Med.* 2016;30:421–429.

34. Villain N, Desgranges B, Viader F, et al. Relationships between hippocampal atrophy, white matter disruption, and gray matter hypometabolism in Alzheimer's disease. *J Neurosci.* 2008;28:6174–6181.

35. Murray ME, Graff-Radford NR, Ross OA, Petersen RC, Duara R, Dickson DW. Neuropathologically defined subtypes of Alzheimer's disease with distinct clinical characteristics: a retrospective study. *Lancet Neurol.* 2011;10:785–796.

36. Whitwell JL, Dickson DW, Murray ME, et al. Neuroimaging correlates of pathologically defined subtypes of Alzheimer's disease: a case-control study. *Lancet Neurol.* 2012;11:868–877.

37. Whitwell JL, Jack CR Jr, Kantarci K, et al. Imaging correlates of posterior cortical atrophy. *Neurobiol Aging.* 2007;28:1051–1061.

38. Whitwell JL, Weigand SD, Shiung MM, et al. Focal atrophy in dementia with Lewy bodies on MRI: a distinct pattern from Alzheimer's disease. *Brain.* 2007;130:708–719.